

N94-34195

## SQUEEZE FILM DAMPERS WITH OIL HOLE FEED\*

P.Y.P. Chen and E.J. Hahn  
The University of New South Wales  
Kensington, Australia

77-37  
12863  
7-12  
1

To improve the damping capability of squeeze film dampers, oil hole feed rather than circumferential groove feed is a practical proposition. However, circular orbit response can no longer be assumed, significantly complicating the design analysis. This paper details a feasible transient solution procedure for such dampers, with particular emphasis on the additional difficulties due to the introduction of oil holes. It is shown how a cosine power series solution may be utilised to evaluate the oil hole pressure contributions, enabling appropriate tabular data to be compiled. The solution procedure is shown to be applicable even in the presence of flow restrictors, albeit at the expense of introducing an iteration at each time step. Though not of primary interest, the procedure is also applicable to dynamically loaded journal bearings with oil hole feed.

## NOMENCLATURE

$a_j$	radius of $j$ 'th oil hole
$C$	radial clearance
$D$	bearing or journal diameter
$d_j$	diameter of $j$ 'th oil hole
$h$	film thickness; $H = h/C$
$L$	bearing land length
$M, N$	summation integers
$n$	number of oil holes
$P$	gauge pressure relative to cavitation pressure; $P = pC^2 / (12\mu\Omega L^2)$
$P^*$	defined by eqn. (7)
$P_i, P_o$	inlet and outlet gauge pressures
$P_s, P_c$	solutions to eqns. (8) and (9) respectively
$P_j$	solution to eqn. (12)
$P_{oj}$	non-dimensional pressure at the $j$ 'th oil hole
$P_{ss}$	non-dimensional supply pressure
$R$	bearing or journal radius
$r$	non-dimensional radial coordinate; $r = \rho/a_j$
$t$	time; $\tau = \Omega t$
$U, V$	relative velocities of the bearing surfaces in the $X, Y$ directions at angular location $\theta$ in Figure 1

\* The work reported herein was supported by an Australian Research Council grant.

$X, Y, Z$	coordinates located in centre plane of bearing at intersection of the line of centres $O_b O_j$ with the bearing surface as shown in Figure 1; $\bar{Z} = Z/L$
$X_j$	X coordinate of the j'th oil hole
$\alpha_{ij}$	series coefficients defined by eqn. (20)
$\theta$	angular location of the point A from the line of centres along the bearing surface as shown in Figure 1; $\theta = X/R$
$\theta_j$	angular location of the j'th oil hole; $\theta_j = X_j/R$
$\mu$	mean viscosity of lubricant
$\rho, \psi$	polar coordinates with origin at centre of j'th oil hole as shown in Figure 3
$\rho$	unbalance eccentricity in Figure 1
$\Delta_j$	time dependent multiplier of $P_j$
$\chi_j$	defined by eqn. (19)
$\phi$	angular displacement of the line of centres from the vertical direction as shown in Figure 1.
$\eta$	a constant; $\eta = 1$ for journal bearings, $\eta = 0$ for dampers
$\Omega$	$\omega_b + \omega_j$
$\omega_{b,j}$	angular velocity of bearing and journal respectively
$\lambda_j$	$L/d_j$
.	denotes differentiation with respect to time $\tau$

## INTRODUCTION

Because of their compact size and wide range of damping capability, squeeze film dampers are frequently used for stabilisation and vibration attenuation of rotating machinery. Oil feed is generally via a central circumferential groove, effectively splitting the damper width  $L$  into two dampers, each with axial land length of  $L/2$ . However, such a design effectively reduces the damping capability of the damper by a factor of four. To recover this lost damping capability, one can dispense entirely with the circumferential groove feed and introduce all the lubricant from either of the bearing ends. Such a concept requires an axial seal to ensure that the lubricant does not bypass the damper clearance space. A practically more reliable alternative is to introduce the lubricant via one or more (usually two or four) oil holes in the central axial plane of the damper, i.e. replacing the circumferential groove with a number of oil holes. While this arrangement ensures that all the lubricant passes through the damper clearance, the unbalance response analysis for even the simplest case of a squeeze film damped centrally preloaded horizontal rigid rotor or a squeeze film damped vertical rotor has become significantly more complicated. Whereas with the end feed dampers, one can assume circular orbit response in the steady state, such is no longer the

case with oil hole feed dampers where the steady state response generally needs to be obtained by a transient solution. Transient analyses rely heavily on approximations such as the short bearing approximation or compilation of appropriate tabular data, to be computationally feasible, the latter approach being warranted at relatively high aspect ratios ( $L/D > 0.25$ ) and eccentricity ratios ( $\epsilon > 0.7$ ) (Hahn, 1989). Such a tabular approach is expected to be necessary with oil hole feed, so the major emphasis of this paper centres on how to obtain satisfactory tabular data and thereby overcome the added complication due to the introduction of oil hole feed.

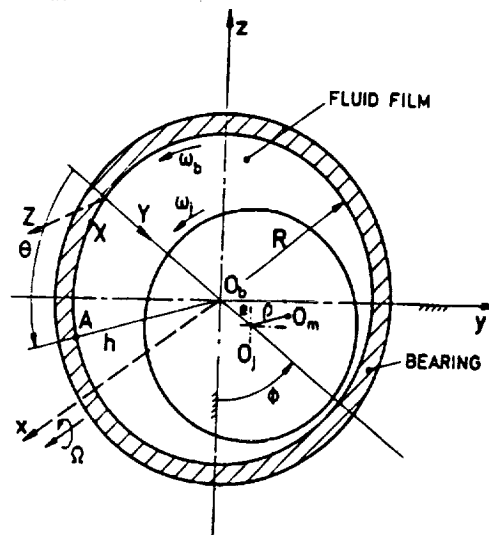


Figure 1: Simple circular bore hydrodynamic bearing or squeeze film damper.

### SOLUTION STRATEGY

Figure 1 depicts a simple circular bore hydrodynamic journal bearing or squeeze film damper if the journal does not rotate (i.e. if  $\omega_j = 0$ ). Figure 2 shows the journal oil feed pressure boundary conditions which now, in addition to specified inlet and outlet pressures  $p_i$  and  $p_o$ , allow for  $n$  oil feed holes at the centre plane of the bearing (i.e. along  $Z = 0$ ). For the usual assumptions of laminar flow, Newtonian fluid, constant fluid properties, negligible inertia force, body force and curvature effects, no slip at bearing surfaces, no axial variation in film thickness, constant pressure across the film and validity of order of magnitude considerations, one can derive the Reynolds equation as (Pinkus and Sternlicht, 1961):

$$\frac{\partial}{\partial X} \left( h^3 \frac{\partial p}{\partial X} \right) + h^3 \frac{\partial p}{\partial Z^2} = -6\mu U \frac{\partial h}{\partial X} + 12\mu V, \quad (1)$$

where

$$h = (C + \epsilon \cos\theta) \quad (2)$$

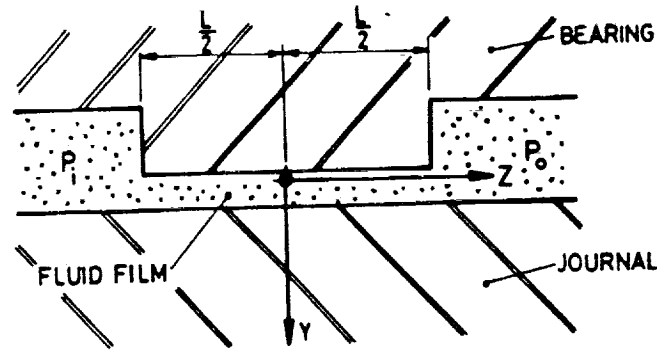


Figure 2: Bearing or damper with end feed and end drain pressure boundary conditions.

The boundary conditions pertaining to eqn. (1), as shown in Figure 2, are:

$$\begin{aligned} p &= p_i \text{ at } Z = -L/2 \\ p &= p_o \text{ at } Z = L/2 \end{aligned} \quad (3)$$

These boundary conditions describe end feed conditions. Additionally, there are now  $n$  circumferentially equispaced oil holes in the mid circumferential plane at  $Z = 0$ , supplied from an oil chamber at supply pressure  $p_s$ . Finally, the pressure distribution is periodic in the circumferential (i.e.  $\theta$ ) direction with period  $2\pi$ .

Then, in non-dimensional form

$$\frac{L^2}{R^2} \frac{\partial}{\partial \theta} \left( H^3 \frac{\partial P}{\partial \theta} \right) + H^3 \frac{\partial^2 P}{\partial Z^2} = \epsilon \left( \dot{\phi} - \frac{\eta}{2} \right) \sin \theta + \dot{\epsilon} \cos \theta \quad (4)$$

where  $H = (1 + \epsilon \cos \theta)$  . (5)

Ignoring for the time being the problem of cavitation, the solution of eqn. (3) may be written as

$$P = \epsilon \left( \dot{\phi} - \frac{\eta}{2} \right) P_s + \dot{\epsilon} P_c + \left( \frac{P_o - P_i}{2} \right) \bar{Z} + \left( \frac{P_o + P_i}{2} \right) + \Delta_1 P_1 + \Delta_2 P_2 + \dots + \Delta_n P_n \quad (6)$$

$$= P^* + \Delta_1 P_1 + \Delta_2 P_2 + \dots + \Delta_n P_n \quad (7)$$

where  $P_s$  and  $P_c$  are the solutions of

$$\frac{L^2}{R^2} \frac{\partial}{\partial \theta} \left( H^3 \frac{\partial P_s}{\partial \theta} \right) + H^3 \frac{\partial^2 P_s}{\partial Z^2} = \sin \theta \quad (8)$$

and  $\frac{L^2}{R^2} \frac{\partial}{\partial \theta} \left( H^3 \frac{\partial P_c}{\partial \theta} \right) + H^3 \frac{\partial^2 P_c}{\partial Z^2} = \cos \theta \quad (9)$

respectively, with boundary conditions  $P_s = P_c = 0$  at  $\bar{Z} = \pm 1/2$ , (10)

and  $P_s(\theta) = P_s(\theta + 2\pi); P_c(\theta) = P_c(\theta + 2\pi);$  (11)

and where  $P_j (j = 1, 2, \dots, n)$  are given by the solutions of:

$$\frac{L^2}{R^2} \frac{\partial}{\partial \theta} \left( H^3 \frac{\partial P_j}{\partial \theta^2} \right) + H^3 \frac{\partial^2 P_j}{\partial \bar{Z}^2} = 0, \quad (12)$$

with boundary conditions:  $P_j = 0$  at  $\bar{Z} = \pm 1/2$ , (13)

and  $P_j = 1$  at  $\bar{Z} = 0, \theta = \theta_j.$  (14)

In eqns. (6) and (7), the  $\Delta_j$ 's are time dependent multipliers so that at any instant of time, at  $\bar{Z} = 0$  and  $\theta = \theta_j$

$$\Delta_1 P_1 + \Delta_2 P_2 + \dots + \Delta_n P_n = P - P^* = P_{oj} - P^* \quad (15)$$

Strictly speaking, this formulation implies that the pressure will be  $P_{oj}$  at the centre of the oil hole but may be somewhat different from this elsewhere; whereas in fact the pressure should equal  $P_{oj}$  everywhere within the oil hole region. The error due to this assumption will increase as the hole diameter  $d_j$  increases but owing to the near parabolic axial profiles of  $P_s$  and  $P_c$ , is expected to have insignificant effect for  $\lambda \leq 6$ .

If there is flow restriction between the supply pressure  $P_{ss}$  and the pressure at the hole at  $\theta = \theta_j$ , e.g. a capillary or orifice, one needs in general to balance the flow through the restrictor to the flow out of the oil hole. To cater for such an eventuality, an iteration is introduced whereby the hole pressures  $P_{oj}$  are guessed and subsequently modified until there is flow balance. Eqn. set (15) then constitutes a set of  $n$  simultaneous linear equations in the  $n$  unknowns  $\Delta_1, \dots, \Delta_n$ . If the restrictors offer sufficiently small resistance to the flows, the pressure drop across them will be negligible, whereupon all  $P_{oj} = P_{ss}$  and the need for iteration is avoided. In any case, eqn. (6) gives, for this instant of time, the full pressure distribution around the damper. Such an approach allows for fluid to be pumped out as well as sucked in at the holes. Such pump out would in practice be avoided by using a check valve. In such a case, whereas the pressure can never fall below  $P_{ss}$  at any oil hole, any respective hole can be ignored once  $P^*$  exceeds  $P_{ss}$ , thereby reducing the number of 'effective' oil holes  $n$ .

The major computational problem involves obtaining the pressure distributions  $P_s, P_c$  and  $P_j$  at each instant of time. It is computationally prohibitive to solve numerically the partial differential equations (8), (9) and (12) at each instant of time, so a data tabulation/interpolation strategy is adopted. As may be seen from eqns. (8) - (11),  $P_s$  and  $P_c$  are, for a given aspect ratio  $L/R$ , functions of  $\theta, \bar{Z}$  and  $\epsilon$ . Three dimensional arrays for  $P_s$  and  $P_c$  with sufficient elements to allow accurate interpolation are both impractical and unnecessary for, as shown in Rezvani and Hahn (1992), by assuming a parabolic shape for the  $P_s$  and  $P_c$  in the axial direction, two dimensional arrays which are functions of  $\theta$  and  $\epsilon$  only will suffice with adequate accuracy for aspect ratios as high as  $L/D = 1$ , and eccentricity ratios as high as  $\epsilon = 0.9$ , or even higher.

The same cannot, unfortunately, be said for any of the  $P_j$  pressure distributions, since they are a function of the  $j$ 'th oil hole location  $\theta_j$  with respect to the line of centres, which

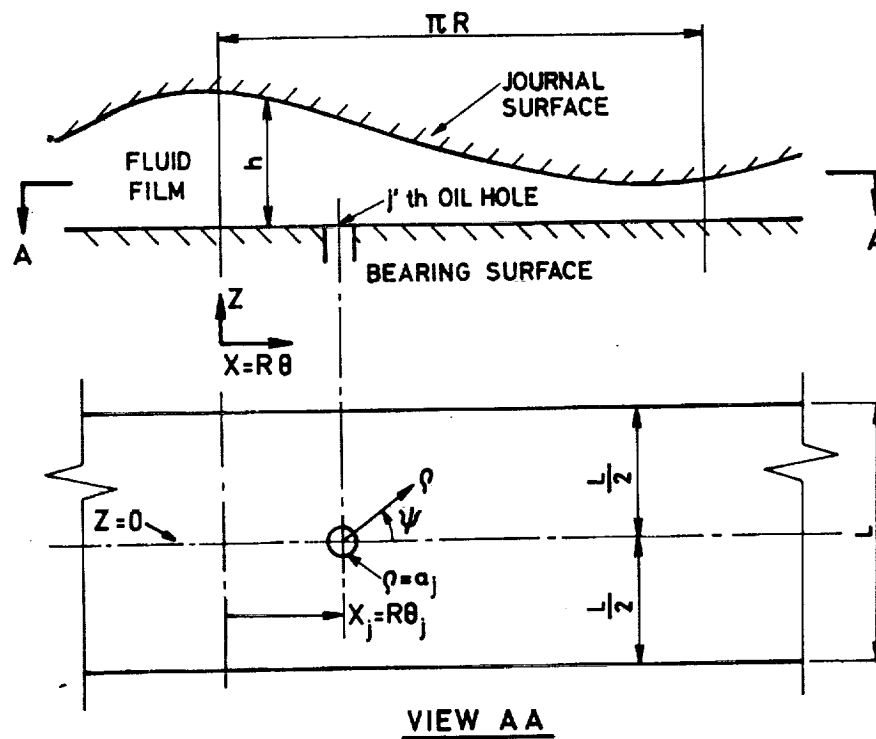


Figure 3: Laid out journal bearing or damper with oil hole at  $\theta = \theta_j$ .

location changes with time. Figure 3 depicts the laid out journal bearing or damper with the instantaneous location of the oil hole at  $\theta_j$ . Attention can be restricted to the solution for  $P_j$  for a single oil hole, since the value of  $\theta_j$  is arbitrary and can therefore apply to any of the

oil holes. Thus a sufficient number of  $P_j$  distributions need to be stored, to enable  $P_j$  to be found with sufficient accuracy at any time by interpolation. Additionally, the  $P_j$  are also functions of  $\theta, \bar{Z}$  and  $\epsilon$  suggesting the need for four dimensional arrays. Nor can they be found by approximate or numerical solution as easily as the  $P_s$  and  $P_c$ , owing to the finite size of the oil holes, and indeed the size of the axial width of the bearing land relative to the hole diameter  $\lambda_j$  is a parameter which is likely to have a significant effect. For finite sized oil holes, numerical solution of eqn. (12) using finite differences is awkward, owing to the mix of curved and straight boundaries. Thus, Marmol and Vance (1978) assume the oil holes to be smaller than the finite difference mesh. Not that a finite difference solution would solve the tabulation problem since at any instant of time, the  $P_j$ 's would be functions not only of  $\theta, \bar{Z}$  and  $\epsilon$  but also of  $\theta_j$ . Nor has a satisfactory approximate solution approach been found. Rather, a cosine power series solution approach, described below, has been found to be satisfactory and promises to provide manageable tabulation data.

Once all the pressure distribution components have been found, the full pressure distribution  $P$  can be found from eqn. (6). Cavitation can then be approximated by setting  $P = 0$  when  $P < 0$ , a commonly adopted assumption in transient analysis, as the insistence of zero pressure gradient at the cavitation boundary would unduly prolong the time required to evaluate the pressure distribution, and hence, the fluid film forces, whereas the resulting gain in accuracy is expected to be minimal.

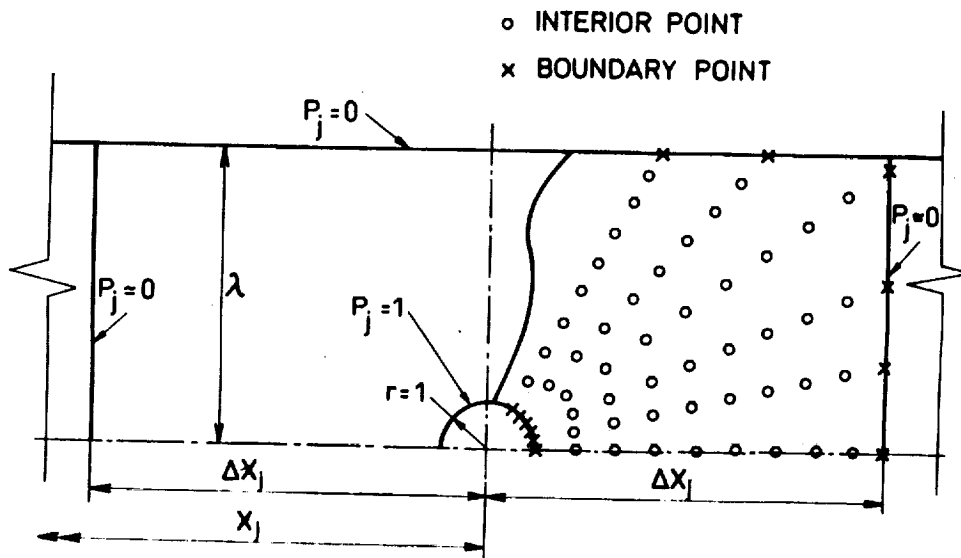


Figure 4: Solution domain for  $P_j$  ( $M = 10, N = 16$ ).

## COSINE POWER SERIES SOLUTION FOR $P_j$

Required is the solution of

$$\frac{\partial}{\partial X} \left( H^3 \frac{\partial P_j}{\partial X} \right) + \frac{\partial}{\partial Z} \left( H^3 \frac{\partial P_j}{\partial Z} \right) - \nabla \cdot H^3 \nabla P_j = 0 \quad (16)$$

over the domain in Figure 4, where  $P_j = 0$  at  $Z = \pm L/2$ ,  $P_j = 1$  around the circumference of a circle of radius  $a_j$  centred at  $Z = 0, \theta = \theta_j$ .

The circular boundary formed by the oil hole, suggests the reformulation of eqn. (16) in terms of polar coordinates  $(r, \psi)$ . With origin of these coordinates at the centre of the oil hole, eqn. (16) may be written as:

$$\frac{\partial^2 P_j}{\partial r^2} + \frac{1}{r} \frac{\partial P_j}{\partial r} + \frac{1}{r^2} \frac{\partial^2 P_j}{\partial \psi^2} + 3 \left( \frac{\partial P_j}{\partial r} \frac{\partial \ln H}{\partial r} + \frac{1}{r^2} \frac{\partial P_j}{\partial \psi} \frac{\partial \ln H}{\partial \psi} \right) = 0 \quad (17)$$

where  $H = 1 + \epsilon \cos \theta = 1 + \epsilon \cos \chi_j \quad (18)$

and where  $\chi_j = \theta_j + \frac{a_j r}{R} \cos \psi = \theta_j + \frac{rL}{\lambda_j D} \cos \psi \quad (19)$

Thus,  $\chi_j$  is a function of  $r, \psi, \lambda_j, L/D$  and  $\theta_j$ .

Hence, for a given bearing with given  $L/D$  and  $\lambda_j$ , the  $P_j$  at any instant of time will depend on  $\epsilon$  and  $\theta_j$ . Generally, all  $n$  holes would have equal diameters, so that henceforth  $\lambda_j = \lambda$ .

In view of the symmetry about  $Z = 0$ , a cosine power series solution approach is adopted. Letting

$$P_j = \sum_{i=1}^M \sum_{j=1}^N \alpha_{ij} r^{i-1} \cos(j-1)\psi \quad (20)$$

where the integers  $M$  and  $N$  are chosen sufficiently large to assure convergence. Substitution into eqn. (17) and evaluation of eqn. (17) at selected points within the solution domain and along the curved, the 'side' and the 'end' boundaries results in  $MN$  simultaneous equations, for the  $MN$  unknowns  $\alpha_{ij}$ .



## RESULTS AND DISCUSSION

The points selected were along rays as shown in Fig. 4. Each ray was subdivided into 9 equal segments between the oil hole and an outer boundary, so that  $M = 10$  in Eqn. (20). In this regard, since the precise boundaries to the left and right are unspecified and may be assumed to extend indefinitely, the solution is restricted to finite distances  $\pm\Delta X_j$  on either side of  $X_j$  with the value of  $P_j$  set to 0 at these boundaries. To ensure that the solution was virtually asymptotic at  $\pm\Delta X_j$ ,  $\Delta X_j$  is increased until no readily discernible difference occurred in the respective solutions.

Using 16 such equispaced 'rays', so that  $N = 16$  in eqn. (20), resulted in 160 linear simultaneous equations for the 160 values of  $\alpha_{ij}$ . This was to give sufficient accuracy for the parameter combinations tested. Also, definition of the side boundaries by selecting a  $\Delta X_j$  of four hole diameters was generally found to be adequate for  $\lambda = 6$ . Since eqn. (16) is simply Laplace's equation if  $H$  is constant, the accuracy of this solution procedure (for constant  $H$ ) was able to be tested against an existing single series solution procedure described in the literature (Takeuti and Sekiya, 1968), and was found to be in agreement.

To illustrate the variation of the  $P_j$  with  $\epsilon$  and  $\theta_j$ , Figs. 5 to 10 give the solutions for  $\epsilon = 0.5$  and 0.9, with  $\theta_j = 0^\circ, 90^\circ$  and  $180^\circ$  for a bearing with  $L/D = 0.5$  and  $\lambda = 6$ . As expected, for  $\theta_j = 0^\circ$  and  $180^\circ$ , (Figs. 5, 7, 8 and 10) the solution is symmetrical about the vertical centreline, but the pressure contours are skewed for the other  $\theta_j$ . Maximum skewness would occur around  $\theta_j = 90^\circ$ , and for  $\epsilon = 0.9$  (Fig. 9) one would probably need to further increase  $M$ ,  $N$  and the  $\Delta X_j$  to improve the accuracy of the small values of  $P_j$ .

Since  $\theta_j$  is solution dependent, data for a sufficient number of discrete  $\theta_j$  values will need to be provided to allow for interpolation in a transient programme. A comparison of Figs. 5 and 8, 6 and 9, and 7 and 10 illustrates the variability of the solutions with  $\epsilon$ . Again, since  $\epsilon$  is solution dependent, data for a sufficient number of discrete  $\epsilon$  values will need to be provided to allow for interpolation. However, rather than store the  $P_j$  pressure distributions for a range of values of  $\epsilon$  and  $\theta_j$ , it will be sufficient to store the  $\alpha_{ij}$  coefficients, thereby

significantly reducing data storage requirements, e.g. data for 10 discrete values of  $\theta_j$  and 20 discrete values of  $\varepsilon$  would appear feasible.

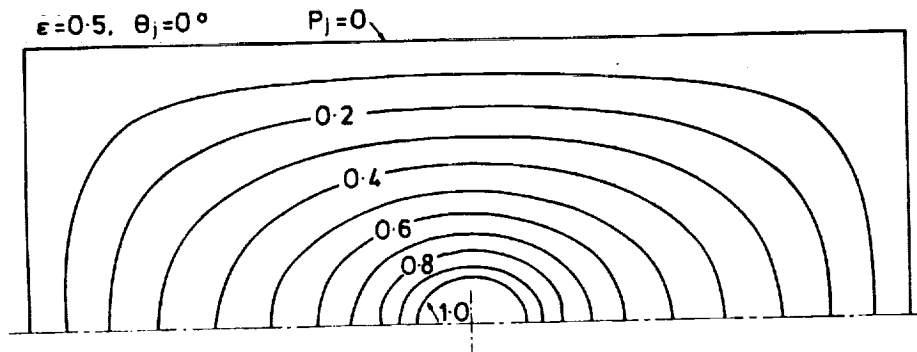


Figure 5: Solution for  $P_j$  for  $\lambda = 6, \varepsilon = 0.5, \theta_j = 0^\circ$ .

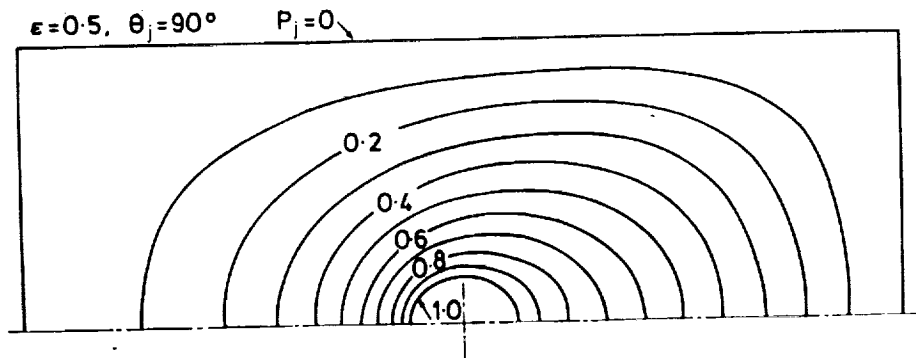


Figure 6: Solution for  $P_j$  for  $\lambda = 6, \varepsilon = 0.5, \theta_j = 90^\circ$ .

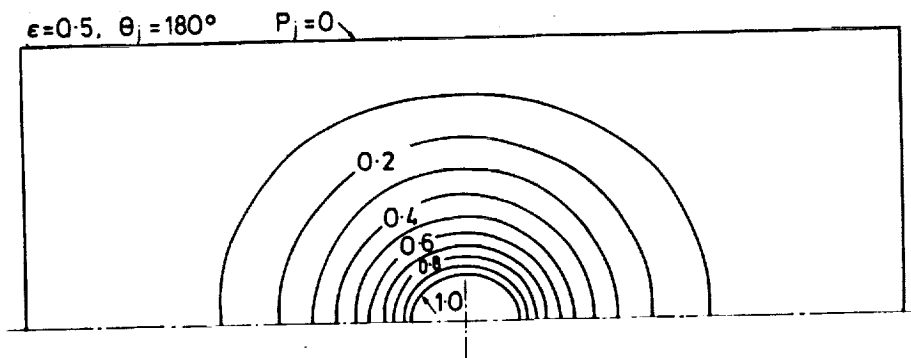


Figure 7: Solution for  $P_j$  for  $\lambda = 6, \varepsilon = 0.5, \theta_j = 180^\circ$ .

Similar results were obtained for larger and smaller oil hole diameters (i.e. larger and smaller values of  $\lambda$ ). Since the pressure drops relatively rapidly, interaction between the  $P_j$

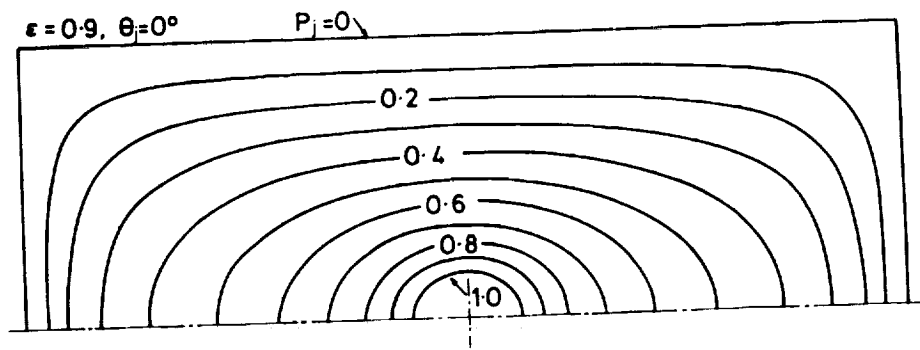


Figure 8: Solution for  $P_j$  for  $\lambda = 6, \epsilon = 0.9, \theta_j = 0^\circ$ .

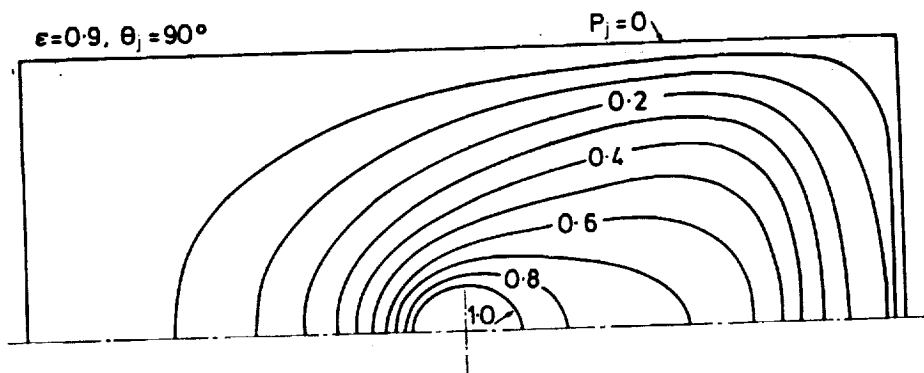


Figure 9: Solution for  $P_j$  for  $\lambda = 6, \epsilon = 0.9, \theta_j = 90^\circ$ .

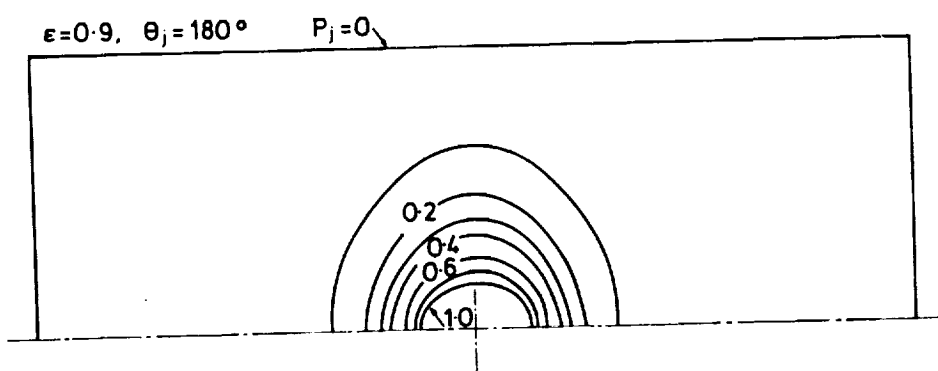


Figure 10: Solution for  $P_j$  for  $\lambda = 6, \epsilon = 0.9, \theta_j = 180^\circ$ .

pressure contributions from other oil holes is negligible until the number of oil holes is so large that neighbouring centres are within 5 oil hole diameters of each other, (e.g. for  $\lambda = 6$  and  $L/D = 0.5$ , such interaction could be neglected provided there were fewer than about 8 oil holes). Hence, in most practical situations, it is expected that such interaction is negligible, so that eqn. (15) simplifies to:

$$\Delta_j P_j = P - P^* = P_{ss} \quad (21)$$

at  $\bar{Z} = 0$  and  $\theta = \theta_j$ . This ability to treat oil holes independently also considerably simplifies the iteration introduced in the case of a flow restriction between supply reservoir and the hole exit.

### CONCLUSIONS

- (a) A feasible computational strategy for the transient solution of dynamically loaded bearings or dampers with oil hole feed has been outlined, relying on interpolation from previously computed data.
- (b) The procedure allows for any number of oil holes, allows for the provision of check valves to avoid pump out and allows for oil flow restriction between the supply reservoir and the oil hole, albeit at the expense of an added iteration.
- (c) The pressure contributions due to the oil holes may be conveniently obtained using a cosine power series solution.
- (d) Such solutions are eccentricity and oil hole location (relative to line of centres) dependent at any instant of time.
- (e) The solutions prove that there is no significant interaction between the pressure contributions of adjacent holes, provided they are spaced at least four oil hole diameters apart. This would pertain in most if not all practical applications.
- (f) The solution procedure is here restricted to the oil holes being located in the central circumferential plane. For off-centred oil holes, the series would need to include sine terms as well. This extension is not expected to create any undue difficulties.

### REFERENCES

- Hahn, E. J., 1989, "Approximate Solution Techniques for Dynamically Loaded Narrow Hydrodynamic Bearings", *Mech. Engg. Transactions, I.E.Aust.*, Vol. ME14, No.3, pp.134-140.
- Marmol, R. and Vance, J., 1978, "Squeeze Film Damper Characteristics for Gas Turbine Engines", *ASME Journal of Mechanical Design*, Vol. 100, pp.139-146.
- Pinkus, O. and Sternlicht, B., 1961, "Theory of Hydrodynamic Lubrication", McGraw Hill, N.Y.
- Rezvani, M. and Hahn, E. J., 1992, "Limitations of the Short Bearing Approximation in Dynamically Loaded Narrow Hydrodynamic Bearings". Presented at 1992 ASME/STLE Tribology Conference. To be published in *ASME Journal of Tribology*, = 7pp.
- Takeuti, Y. and Sekiya, T., 1968, "Thermal Stresses in a Polygonal Cylinder with a Circular Hole Under Internal Heat Generation", *Zeits. fur Angew. Mech. Math.*, Bd.48, Ht.4, pp.237-246.